Zooplankton fecal pellet flux drives the biological carbon pump during the winter–spring transition in a high-Arctic system

Gérald Darnis [1]*, Maxime Geoffroy,[1,2] Malin Daase,[2,3] Catherine Lalande,[4,5] Janne E. Søreide,[3] Eva Leu,[6] Paul E. Renaud,[3,6] Jørgen Berge[2]

[1]Centre for Fisheries Ecosystems Research, Marine Institute of Memorial University of Newfoundland, St. John's, Newfoundland, Canada
[2]Department of Arctic and Marine Biology, Faculty of Biosciences, Fisheries and Economics, UiT The Arctic University of Norway, Tromsø, Norway
[3]The University Centre in Svalbard, Longyearbyen, Norway
[4]Amundsen Science, Université Laval, Québec, Canada
[5]Division of Ocean and Atmospheric Science, Korea Polar Research Institute, Incheon, Republic of Korea
[6]Akvaplan-niva, Fram Centre for Climate and the Environment, Tromsø, Norway

Abstract

Recent research highlighted significant marine biological activity during the Arctic winter, with poorly known implications for the biological carbon pump. We used moored instruments to (1) track the development of the pelagic food web of a high-Arctic marine ecosystem from winter to spring, and (2) assess the role of zooplankton-mediated processes in the sinking export of particulate organic carbon (POC). Zooplankton collected by a sediment trap at 40 m depth in Kongsfjorden showed a shift in species composition in February coinciding with an inflow of Atlantic water and the return of sunlight. The Atlantic copepod *Calanus finmarchicus* and the Arctic *Calanus glacialis* became dominant in the post-inflow assemblage of large mesozooplankton. However, large copepods were never abundant (0.3–4.6 ind m^{-3}) in January–April in the upper 40 m. Despite the low chlorophyll fluorescence, POC export increased substantially, from 2–13 mg C m^{-2} d^{-1} in January–February to 13–35 mg C m^{-2} d^{-1} in March–April 2014. By late March, zooplankton fecal pellets contributed largely (23–100%) to this significant POC export before the phytoplankton bloom. The lack of change in copepod and euphausiid population sizes suggests that enhanced feeding activity in the surface layer supported the increasing fecal pellet export. Our results revealed the swift response of active zooplankton in winter, evidenced by increased carbon export, to improved food availability.

During the polar night, darkness and freezing temperatures restrict biological production in the pelagic zone of the Arctic Ocean (Hegseth et al. 2019). Recent studies have shown, nonetheless, that key components of the Arctic marine food web are active, even during the polar night and the remaining months of the Arctic winter, when extremely low ambient light levels prevail (Berge et al. 2015*a*, 2020). From the base of the high-Arctic pelagic food web to the top, organisms with highly sensitive photoreceptors function at light levels not perceptible by the human eye, nor by standard oceanographic optical sensors (Cohen et al. 2015). Data from autonomous biogeochemical ARGO floats and winter in situ chlorophyll *a* (Chl *a*) measurements revealed net growth of phytoplankton as early as February under 100% sea ice concentration in Baffin Bay and in ice-free Kongsfjorden (Randelhoff et al. 2020; Hoppe 2022). Seabirds and fish were also found to forage in the polar night in Kongsfjorden (Berge et al. 2015*a*). However, the biogeochemical role of the biological activity during the wintertime and prebloom period (i.e., winter biological pump) is still poorly understood in the Arctic.

*Correspondence: gerald.darnis@qo.ulaval.ca

Additional Supporting Information may be found in the online version of this article.

Author Contribution Statement: GD, MG, MD, and CL conceptualized the research. GD, MG, MD, JES, PR, EL, and JB collected samples and raw data. GD, MG, and MD processed the samples and the data. GD did visualization. GD and MG analyzed the data. GD, MG, PER, and JB did funding acquisition. GD wrote the original draft of the manuscript. All authors edited and approved the final version of the manuscript.

Zooplankton-mediated processes play a critical part in the biogeochemical cycling of elements in marine ecosystems, regulating the efficiency of the biological carbon pump by either enhancing or limiting the downward carbon export from the epipelagic zone (Halfter et al. 2020; Kiko et al. 2020). Large Arctic herbivorous copepods such as *Calanus* spp. graze heavily on the ice algal and phytoplankton production and, thus, attenuate the sinking of POC (Tremblay et al. 2006). On the other hand, zooplankton repackage small algal cells and detrital matter into larger dense and fast-sinking fecal pellets, of which a fraction escapes degradation in the water column and settles to the seafloor to feed benthic organisms or to be sequestered in the sediments (Fortier et al. 1994). Another vector of carbon export is the active transport to depth through vertical migrations of macrozooplankton, such as euphausiids (Darnis et al. 2017) and large lipid-rich copepods, that activate the "lipid pump" (Jónasdóttir et al. 2015). Therefore, knowledge of plankton communities, their metabolism, and trophic interactions is critical to understand carbon pathways in marine ecosystems.

The alarming rate of Arctic warming, nearly four times faster than in the rest of the world since 1979 (Rantanen et al. 2022), results in major disruptions to the functioning of the Arctic marine ecosystem as a whole. The rapid decline in sea ice extent and thickness is dramatically changing the light regime, nutrient supply, algal phenology, and pelagic primary productivity (Ardyna et al. 2020), with expected cascading effects on higher trophic levels and on the biogeochemical fluxes from pelagic biological processes. The northward expansion of boreal plankton transported with the increasingly warm inflow of Atlantic- and Pacific-origin waters leads to a borealization of the Arctic seas (Shu et al. 2022), which is altering the pelagic community structure and food web properties, especially in the two main Arctic gateways, namely the Fram Strait and the Bering Strait (Basedow et al. 2018; Oziel et al. 2020; Polyakov et al. 2020). To better predict the impacts of Arctic warming on biogeochemical fluxes, it is necessary to improve our understanding of the mechanisms involved in the transfer of carbon through the pelagic food web and to the ocean depths and the seafloor. This is especially true during the much-understudied winter–spring transition period.

Previous studies indicated that seasonal increases in POC export, in the form of algal aggregates and zooplankton fecal pellets, are prompted by increased microalgal production leading to the spring bloom under favorable conditions (Lalande et al. 2016; Dybwad et al. 2022). Here, we measure the zooplankton contribution to the sinking export of POC during the winter in a high-Arctic fjord influenced by periodic Atlantic-origin water inflow. This study follows previous research that documented the active transport to depth of carbon by zooplankton DVM in Kongsfjorden (Darnis et al. 2017). Moored autonomous instruments, including a sequential sediment trap, in situ fluorescence and photosynthetically active radiation (PAR) sensors, and an acoustic zooplankton fish profiler (AZFP), enabled us to track the seasonal development of biological activity, zooplankton biomass, and POC export out of the epipelagic layer at a high temporal resolution during the winter–spring transition period.

Methods

Study area

Several review studies provided a thorough analysis of the environmental setting and ecosystem in Kongsfjorden (Hop et al. 2002; Svendsen et al. 2002; Hop and Wiencke 2019). Briefly, Kongsfjorden is a glacial fjord comprising two main basins separated by a 30-m deep sill (Svendsen et al. 2002). Three large tidewater glaciers calve into the inner basin, providing a major source of freshwater and terrigenous material to the fjord (Tverberg et al. 2019). The warm West Spitsbergen Current (WSC) and the colder fresher Arctic water from the coastal Spitsbergen Polar Current (SPC) (Fig. 1) influence the hydrography in Kongsfjorden (Tverberg et al. 2019). The dual influence of the WSC and the SPC results in a mix of boreo-Atlantic and Arctic phytoplankton and zooplankton taxa in Kongsfjorden (Basedow et al. 2004; Hegseth et al. 2019; Hop et al. 2019).

At around 79°N, the sun remains below the horizon from 24 October to 18 February in Kongsfjorden. The timing and length of the period of enhanced biological production are driven by numerous environmental factors, including light levels, occurrence of sea ice, winter advection of nutrient-rich water masses, and mixing and stratification processes (Hegseth et al. 2019). During the years 2002–2014, the onset of the phytoplankton bloom varied within a period extending from April to June. The year 2014 was characterized by low in situ Chl *a* fluorescence during spring, and an exceptionally late bloom in June, well after the completion of our sampling in early April (Darnis et al. 2017; Hegseth et al. 2019).

Sampling was done in the outer basin of Kongsfjorden at or close to the station KB3, regularly sampled by different projects (Fig. 1).

Mooring-based autonomous sampling and analysis

Two oceanographic moorings with several autonomous instruments were deployed from early October 2013 to September 2014 (Mooring 1) and from January 2014 to early April 2014 (Mooring 2), respectively, near Sta. KB3 at depths > 200 m (Fig. 1, Table S1 in the Supporting Information). Seapoint fluorescence and LICOR biospherical PAR sensors were mounted on the Mooring 1 at 37 m depth. These sensors were not calibrated prior to deployment and the raw fluorescence and PAR data were normalized and used as relative values. Several temperature sensors spaced at 10-m intervals on the line of
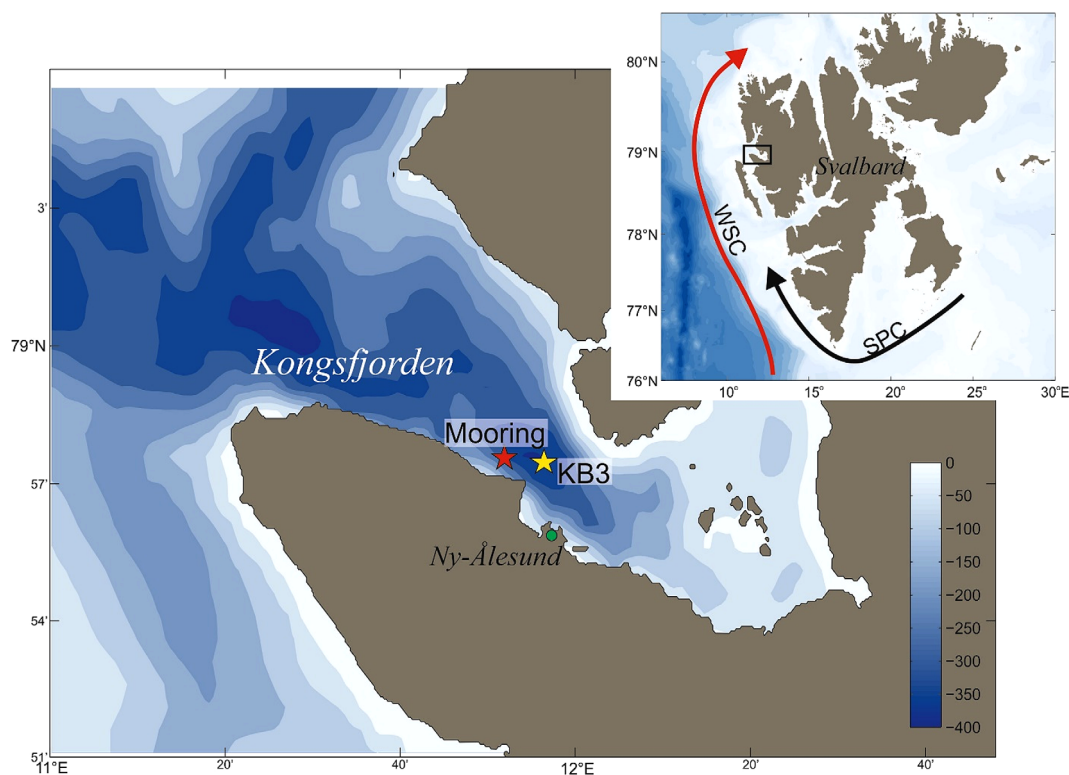
Fig. 1. Location of the mooring site and station KB3 in Kongsfjorden, Svalbard. WSC = West Spitsbergen current; SPC = Spitsbergen polar current.

Mooring 1 recorded seawater temperature at their respective depths between 40 and 210 m.

An upward-looking AZFP (ASL Environmental Science, Victoria, Canada) deployed at 84 m depth on Mooring 2 continuously recorded hydroacoustic data at 125, 200, 455, and 769 kHz from 82 m depth to the surface. Darnis et al. (2017) detailed the AZFP settings and the data analysis process to obtain valid acoustic data from which the abundances of euphausiids and large copepods in the top layer above the sediment trap were derived. In short, bad pings, the backscatter from the sediment trap and the top two meters of the water column were excluded from the analysis. Strong echoes typical of fish schools were also removed from the echograms to keep only the signal from zooplankton. The monthly echogram at each frequency was divided into 1-m vertical by 5-min horizontal echo-integration cells and mean Sv within each cell was exported. A multifrequency analysis was conducted on mean volume backscattering strength (MVBS) and each cell with a frequency response of $MVBS_{125kHz} > MVBS_{200kHz} < MVBS_{455kHz}$ was attributed to euphausiids and $MVBS_{125kHz} < MVBS_{200kHz} < MVBS_{455kHz}$ to copepods. Mean target strength (TS) for each functional group was then estimated based on the randomly oriented fluid bent cylinder model (Stanton et al. 1994). Finally, the backscatter of each functional group was averaged over the top 40 m and the 40-82-m layer and divided by the mean TS to obtain density estimates in ind. m^{-3} with a 1-day temporal resolution. This instrument was calibrated by the manufacturer ($\pm$ 1 dB) prior to deployment (ASL 2014) and the acoustic data processing was performed using the software Echoview 6.0.

A sequential automated sediment trap (McLane PARFLUX Mark78H, 0.5-m^2 collecting area, 21-bottle carousel) was deployed at 100 m depth on Mooring 1. However, a large lump of terrigenous sediment clogged the trap funnel soon after deployment, preventing proper collection of sinking particles for most part of the deployment. A sediment trap identical to the one deployed on Mooring 1 was deployed at 40 m depth on Mooring 2 and intercepted particles from 21 January to 3 April 2014. The 500-mL sample bottles were programmed to rotate at intervals of 3.5 d. Before deployment, the sample bottles were filled with seawater filtered through Whatman GF/F filters (25 mm diameter, 0.7 μm pore size) and with salinity adjusted to 35, using NaCl. The bottles were poisoned with formalin (2% v/v) and buffered with sodium borate to preserve the deposited material. After recovery, each sample bottle was gently sieved through a 125-μm mesh to retain mesozooplankton and larger organisms, all of which were enumerated and identified to the lowest taxonomic level possible. Sinking zooplankton carcasses were not differentiated from zooplankton swimming downward into the trap.

Each sample was then gently sieved through a 60-μm mesh net and the material in the sieve was prepared for zooplankton fecal pellet analysis. The contents were resuspended to a known volume (20–100 mL) depending on the quantity of material in the sample by adding filtered seawater. A 5-mL subsample was drawn, using a pipette with a truncated opening, and poured into a petri dish with a pre-etched grid. Ten to fifteen pictures were taken at 1.6$\times$ magnification with a digital camera mounted on a stereomicroscope. Each picture captured particles within two squares of the grid, corresponding to 7 mm^2 of a petri dish bottom area of 2206 mm^2. Length and width of each fecal pellet or fecal fragment were measured using the open-source program ImageJ (https://imagej.nih.gov/ij/). Volume of the fecal particles was calculated according to their shape. Dense cylindrical pellets were attributed to copepods, larger pieces of cylindrical fecal strings with broken ends to euphausiids, and dense ellipsoid pellets to appendicularians. Total volume of the three main types of fecal particles was estimated based on the number of processed squares, petri dish bottom area, and subsample volume. Fecal pellet carbon was derived from the fecal particle volumes, using volumetric carbon conversion factors of 0.045, 0.031, and 0.026 mg C mm^{-3} for copepod, euphausiid, and appendicularian fecal fragments and pellets, respectively (González and Smetacek 1994; González et al. 1994. Forest et al. 2007; Seuthe et al. 2007; Wexels Riser et al. 2007).

Subsamples for total particulate matter (TPM), POC, and particulate nitrogen (PN) measurements were screened for remaining zooplankton < 60 μm, which were removed before filtration in triplicates through precombusted (450°C for 4 h) and preweighed Whatman GF/F filters (25 mm diameter, 0.7 μm pore size). The filters were rinsed with Milli-Q water to remove salt, and then dried at 60°C for 12 h. The filters were weighed on a microbalance to measure TPM and exposed to concentrated HCl fumes for 12 h to remove inorganic carbon. The filters were folded in tin capsules that were run through a EuroEA3022 elemental analyzer to measure POC and PN.

Zooplankton sampling and analysis

Shipboard sampling and mooring deployments were conducted from the R/V "Helmer Hanssen." The mesozooplankton was sampled using a Hydro-Bios multiple plankton sampler Midi-Multinet with a 0.25-m^2 aperture and fitted with five nets of 180-μm mesh in January, and a WP2 sampler (1-m^2 aperture and 180-μm mesh net) with a net closing mechanism in May. Both samplers were deployed to 320 m depth at Station KB3 and hauled to the surface at 0.5 m s^{-1} for sampling. The sample strata were 320–200 m, 200–100 m, 100–50 m, 50–20 m, and 20–0 m. Four plankton net casts were performed in January and three in May 2014. Samples were preserved in a seawater solution of hexamethylene-buffered 4% formaldehyde until taxonomic analysis. The net samples were rinsed through a 180-μm mesh sieve to remove the formalin.

The zooplankton were then size-fractionated using a 1000-μm mesh sieve and resuspended in freshwater. Known aliquots were taken from the 180–1000-μm size fraction using a 5-mL large tip pipette until > 300 organisms were counted under a stereomicroscope and identified to development stage and to the lowest possible taxonomic level. The > 1000-μm size fraction was processed in its entirety for taxonomic analysis. In contrast to the taxonomic analysis of the zooplankton in the sediment trap samples, *Calanus finmarchicus* and *C. glacialis* were not differentiated in the plankton net samples and were identified as *C. finmarchicus/ glacialis*. Furthermore, all species belonging to the genus *Microcalanus* or *Pseudocalanus* were pooled as *Microcalanus* spp. or *Pseudocalanus* spp., respectively.

Results

Hydrography, light, and chlorophyll fluorescence

The water column was homogeneous from 37 m to the bottom, with temperatures above 0°C for most of the winter until May (Fig. 2a). An increase in water temperature (peaking above 3°C) and salinity (from 34.3 to 34.9) between late January and late February illustrated the first inflow event of Atlantic water (AW) of 2014 in the middle part of Kongsfjorden (Fig. 2a,b). Thermal stratification was established in June and strengthened in early July, long after our trap sampling.

Low PAR values started to be detected by the sensor located at 37 m depth in mid-February and gradually increased from late February to March, before peaking in April (Fig. 3a). Chlorophyll fluorescence started to increase in May and peaked in mid-June (Fig. 3b).
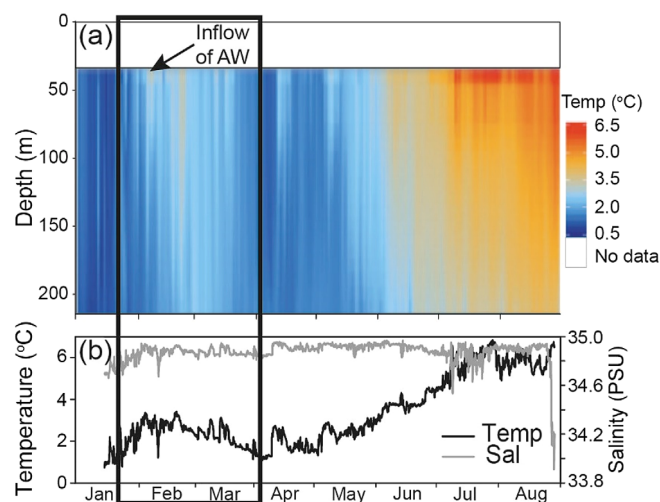

Fig. 2. Time-depth section of (**a**) temperature and (**b**) temperature and salinity at 37 m depth from 17 January to 9 September 2014 in Kongsfjorden. The period of sediment trap-derived particle flux measurement from 21 January to 4 April 2014 is illustrated within the rectangle. AW = Atlantic water
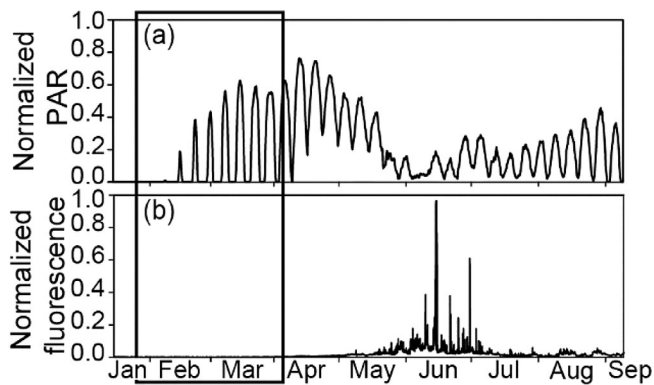
Fig. 3. Time series of (**a**) normalized photosynthetically active radiation (PAR) and (**b**) normalized fluorescence at 37 m depth from 17 January to 9 September 2014 in Kongsfjorden. Each week is represented as a daily average. The period of particle flux measurement is illustrated within the rectangle from 21 January to 4 April.

Zooplankton density and composition

The density of large copepods estimated from the acoustic data in the top 40 m above the sediment trap was variable and low, ranging from 0.3 to 4.6 ind. m^{-3}, from late January to early April (Fig. 4a). In the 40–82 m layer below the trap, the density of large copepods was much higher (range 6–90 ind. m^{-3}) than above the trap and decreased from 47 ± 17 ind. m^{-3} in February to 11 ± 4 ind. m^{-3} in April ($r^2 = 0.06$; $p < 0.05$) (Fig. 4b). The density of euphausiids was also variable in the top layer (Fig. 4c). Ranging from 0 to 0.2 ind. m^{-3}, it was on average 40 times lower than the density of large copepods in that top layer. The density of euphausiids ranged 0.2–5.2 ind. m^{-3} in the 40–82 m layer and was on average 48 times higher than in the layer above (Fig. 4d).

In January, the trap collected few large copepods (3–10 ind. $m^{-2} d^{-1}$) (Fig. 5a), dominated by the Arctic-mesopelagic species *Metridia longa* and *Calanus hyperboreus*, and the boreal-oceanic *Paraeuchaeta* spp. and *C. finmarchicus* (Fig. 5a,b). No

late copepodite stage of the Arctic-shelf species *C. glacialis* was found in the samples during this early part of the study. From the second half of the first week of February onward, the assemblage of large copepods in the trap changed drastically and became largely dominated by late copepodite stages CV-Adult females of the congener *Calanus* species *C. finmarchicus* and *C. glacialis* that accounted for 51% and 47%, respectively, of the large copepods during that period (Fig. 5b). After peaking at 25–27 ind. $m^{-2} d^{-1}$ in the third week of February, the density of large copepods decreased abruptly and did not show any marked trend until the end of sampling.

The number of small- to medium-sized copepods in the trap samples displayed two main peaks above 20 ind. $m^{-2} d^{-1}$ in the third and fourth week of February and one at 15 ind. $m^{-2} d^{-1}$ in the second week of March (Fig. 5c). The density of the small-medium copepod size class at 40 m depth remained within the range of 2–12 ind. $m^{-2} d^{-1}$ during most of the study period. *Oithona similis* and *Pseudocalanus* spp. dominated, representing 41% and 20% of this size class during the study period (Fig. 5c,d). Overall, large and small-medium copepods represented together $82 \pm 13\%$ of the assemblage of zooplankton captured by the trap from January to April.

Few euphausiids were captured throughout the study period (Fig. 5e). The density was 0.3 ind. $m^{-2} d^{-1}$ in the five out of 21 sample bottles that contained euphausiids. However, their passively sinking exuviae were collected in higher numbers from January to late March, peaking at 5 ind. $m^{-2} d^{-1}$ over the first days of February.

The appendicularians *Fritillaria borealis* and *Oikopleura vanhoeffeni* were mainly observed in January and February and their abundance in the trap samples did not exceed 1 ind. $m^{-2} d^{-1}$ when they were present (Fig. 5f). The most abundant microphagous zooplankton, the boreo-arctic *Limacina helicina*, was observed until late March in all but one sample in mid-February. During that period, the density ranged from 0 to 5 ind. $m^{-2} d^{-1}$ and peaked in the last days of January.
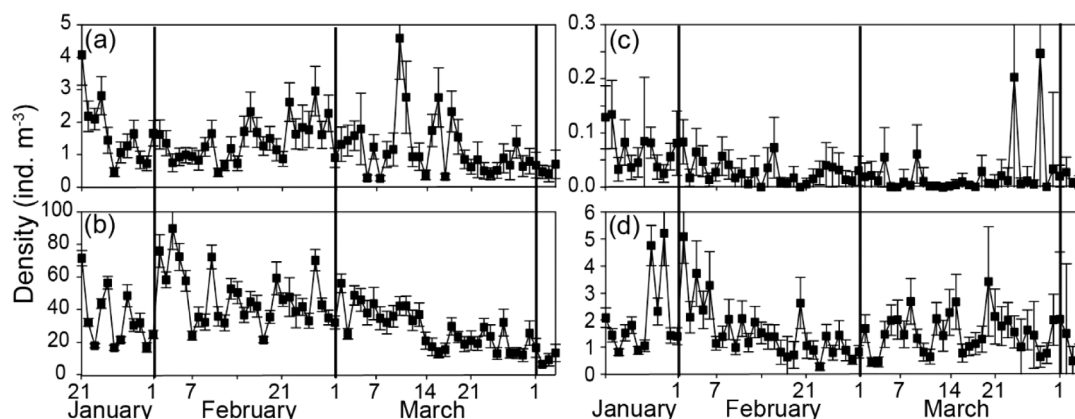

Fig. 4. Time series of acoustically estimated density ($\pm$ 1SE) of large copepods in the (**a**) 2–40 m water layer above the trap and (**b**) 40–82 m layer below the trap, and of euphausiids in the (**c**) 2–40 m and (**d**) 40–82 m layers. Note differences in scales.
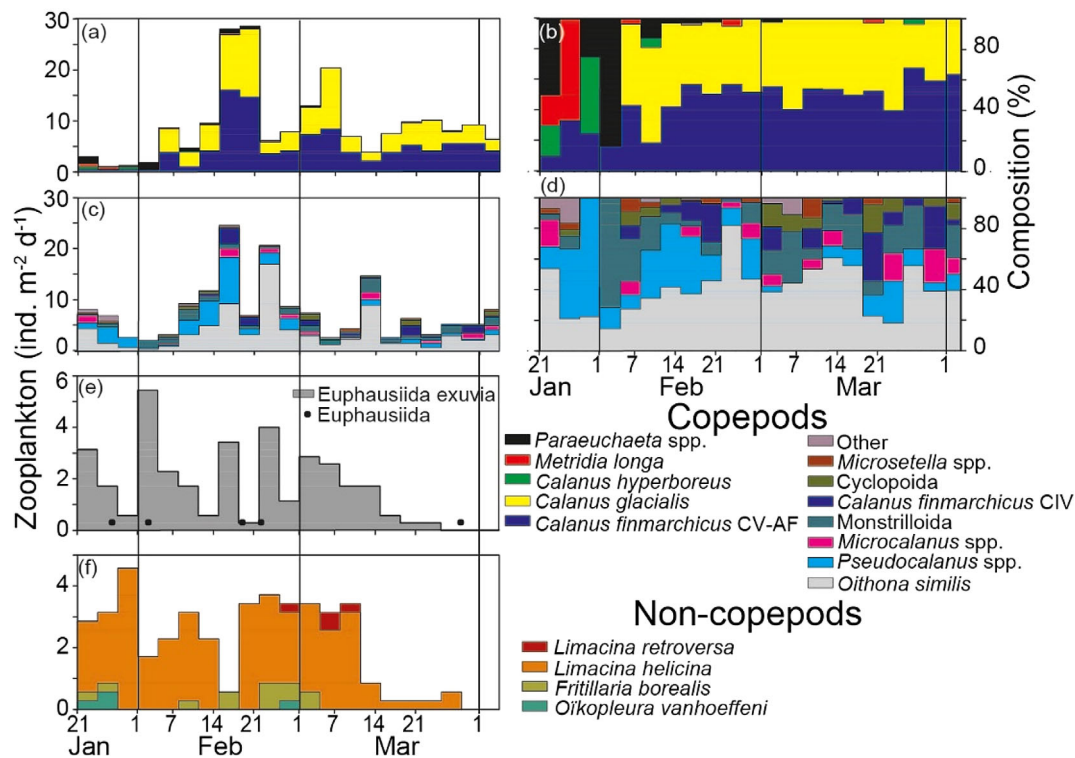
Fig. 5. Time series of abundance and relative contribution of (**a,b**) large and (**c,d**) small-medium size copepods, (**e**) euphausiids and their exuviae, and (**f**) microphagous zooplankton from a sediment trap deployed at 40 m from 21 January to 4 April 2014 in Kongsfjorden. Note differences in scales.

The variability in density of zooplankton eggs showed a temporal pattern different from that of copepod, euphausiid and microphagous zooplankton (Fig. 6). Very few eggs were collected in January and February, but numbers increased in March and peaked in early April (96 eggs m^{-2} d^{-1}). Density of zooplankton larvae was low in the trap samples, reaching a maximum of 3.5 ind. m^{-2} d^{-1} in early April. The low counts of calanoid nauplii (three individuals of *Calanus* spp. and one unidentified calanoid) were made in some of the January–February samples whereas Ophiurida, Cirripedia, and

Fig. 6. Time series of zooplankton eggs and larval stages from a sediment trap deployed at 40 m from 21 January to 4 April 2014 in Kongsfjorden.

Polychaeta larvae were observed in March–April. Larvae of Bivalvia and *Clione limacina* were present during most of the study period.

The four vertical profiles of zooplankton made on 17 and 18 January 2014 indicated that small-medium sized copepods numerically dominated the zooplankton community composition in the water column (88 ± 11%) and in the top layer above the trap (97 ± 3%) (Fig. 7a). Together, *Pseudocalanus* spp., *O. similis*, and *Microcalanus* spp. represented 98 ± 1% of the abundance of the small-medium copepods in the two top strata of the surface layer (433 ± 275 ind. m^{-3}). This size class showed a clear concentration in the top 50 m of the water column. Large zooplankton, including large copepods and euphausiids, were concentrated at depths > 42 m, i.e., below the trap, in January (Fig. 7b,c). *C. finmarchicus/glacialis* represented 81 ± 1% of the density of large copepods (8 ± 5 ind. m^{-3}) in the surface layer above the trap (Fig. 7b). The abundance of euphausiids was extremely low (maximum of 0.8 ind. m^{-3} in the 100–200 m stratum; Fig. 7c). The three profiles made between 12 and 14 May 2014 showed that the zooplankton composition of the two main size classes was similar to the one in January, except for the lesser representation of the neritic *Pseudocalanus* spp. in May (Fig. 7d,e). The abundance of large copepods, integrated over the water column, sampled in May was about 25% lower than sampled in January (Table 1). By contrast, the integrated abundance of the small-medium copepods in May was nearly double the abundance in January. No appendicularian
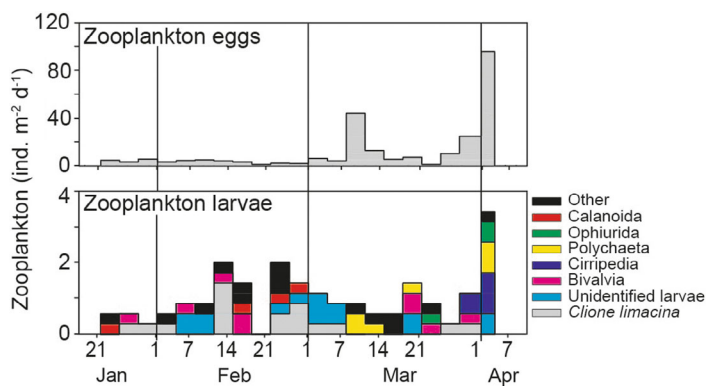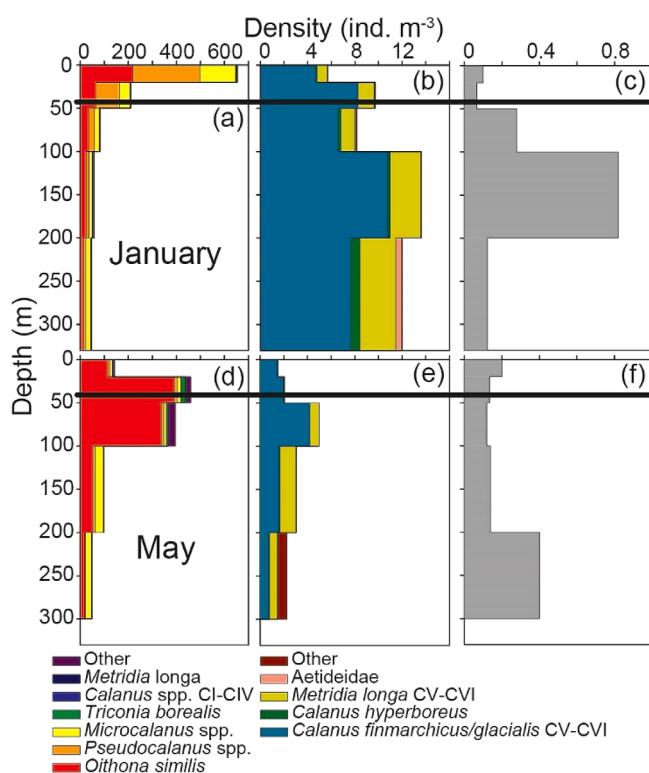
Fig. 7. Vertical distribution of (**a**) small-medium size copepods, (**b**) large copepods, and (**c**) euphausiids in January (top panels) and in May (bottom panels) 2014 at station KB3, close to the mooring in Kongsfjorden, based on plankton net sampling. Black thick horizontal lines indicate trap at 40 m depth.

Fig. 8. Time series of sinking fluxes at 40 m depth of (**a**) total particulate matter (TPM), (**b**) 414 particulate organic carbon (POC), (**c**) krill exuviae, and (**d**) fecal pellet carbon (FPC) from various zooplankton groups from 21 January to 4 April 2014 in Kongsfjorden.

(*F. borealis* or *Oikopleura* spp.) was identified in the net samples in January or May.

Sinking fluxes of particulate matter

The time series of TPM showed a period of low particle flux, never exceeding 1 g m^{-2} d^{-1} in January and February, followed by a period of steady increase through March (Fig. 8a). The TPM flux during the March-early April second phase was 2.4 ± 1.3 (range 1.0–4.6) g m^{-2} d^{-1}, compared with 0.4 ± 0.2 (range 0.02–1.1) g m^{-2} d^{-1} in the earlier phase. The proportion of organic carbon in the sinking particulate matter
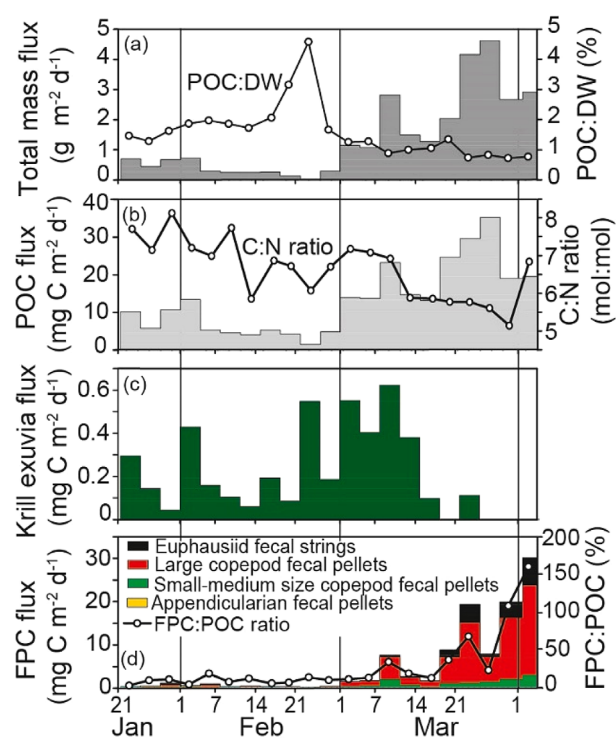
(POC : TPM ratio) ranged from 1.3% to 4.6% during the first period, and from 0.7% to 1.3% during the second period when the ratio decreased over time. The seasonal variability in POC flux displayed a pattern like that of the TPM flux (Fig. 8a,b), generally increasing from March to April (Fig. 8b). The sinking POC was increasingly composed of fresh material from January to April, as indicated by the decreasing C : N ratio.

The flux of POC in the form of krill exuviae represented a small fraction (< 2%) of the total POC flux, except during the last week of February when krill exuviae represented 35% of the low POC flux of 1.5 mg C m^{-2} d^{-1} (Fig. 8c). The krill exuviae flux peaked in the first half of March and then decreased sharply to zero by the end of sampling.

Table 1. Water column-integrated abundance of small-medium and large copepods, and euphausiids in net samples from January and May 2014 at station KB3 close to the mooring in Kongsfjorden. *n* = number of multinet casts.

Month	*n*	Zooplankton group	Mean abundance ± 1 SD (ind m^{-2})
January	4	Small-medium copepods	35,487 ± 6367
		Large copepods	3739 ± 1453
		Euphausiids	116 ± 49
May	3	Small-medium copepods	63,462 ± 27,718
		Large copepods	890 ± 334
		Euphausiids	81 ± 44

The fraction of appendicularian fecal pellet flux was almost negligible and reached a maximum of 5.6% of the FPC flux when the latter was at its second lowest (0.3 mg C m^{-2} d^{-1}) in the first days of trap collection in January (Fig. 8d). The combined FPC flux of euphausiid, large, and small-medium copepods was lowest (0.2 mg C m^{-2} d^{-1}) at the end of February and then increased throughout March to reach a maximum of 31.3 mg C m^{-2} d^{-1} in the last days of collection in early April. The FPC : POC ratio remained below 20% during the January–February period of low POC and FPC fluxes (Fig. 8d). However, the ratio increased steeply in the second half of March and the POC flux in late March and early April was almost entirely made of zooplankton fecal material, as indicated by a ratio > 100%.

Discussion

To better study the productive season at high latitudes, sediment trap studies traditionally increase sampling frequency during the period when phytoplankton blooms occur and reduce it outside this period to monthly or bi-monthly intervals (e.g., Willis et al. 2008; Weydmann et al. 2021; Dybwad et al. 2022). Our continuous collection of sinking material and zooplankton, using a twice-weekly sampling frequency over 10 weeks, revealed a notable rise in particulate organic carbon (POC) export during late winter and early spring, before the bloom. This increase was largely due to zooplankton feeding activity and production of dense fecal pellets (Fig. 8) rather than an increase in zooplankton abundance in the water layer above the trap (Fig. 4). Additional hydrographic data on salinity and temperature, coupled with data on PAR, fluorescence, and zooplankton abundance and vertical distribution, unveiled correlations between the inflow of AW and/or the reappearance of light in Kongsfjorden, with the enhanced zooplankton-mediated POC export occurring well ahead of the phytoplankton bloom. The zooplankton data from the trap also revealed a shift in species composition possibly leading toward more active zooplankton in the surface layer of the study area as early as February.

Winter–spring dynamics of plankton in the surface layer

The southerly winds and the lack of sea ice over the Svalbard western shelf edge in winter 2014 were conducive to surface Ekman drift of AW from the WSC, on top of the denser shelf water, toward Kongsfjorden (Tverberg et al. 2019). Prior to the AW surface inflow event in Kongsfjorden in January–February 2014 (Fig. 2; van de Poll et al. 2016; Hegseth et al. 2019), the major contribution of *M. longa* and *C. hyperboreus* to the low number of large copepods captured in the trap underlined the boreoarctic-mesopelagic status of this size class. Then, the AW inflow most likely transported zooplankton and nutrients across the west Svalbard Shelf into the fjord (Dybwad et al. 2022). Late copepodite stages of the subarctic *C. finmarchicus* and its congener, the Arctic shelf

C. glacialis, became the dominant large copepods (> 80% of the share) in the trap samples during and after the AW advection, until the end of the study period in early April (Fig. 5a). The winter peak of zooplankton density in the trap samples collected at 40 m, 25–27 ind. m^{-2} d^{-1} in the third week of February (Fig. 5a), remained relatively low as it was < 1% of the peak value of > 4000 ind. m^{-2} d^{-1} reached in June 2015 at 60 m depth (Fig. 3 of Weydmann et al. 2021).

Euphausiids and large copepods were identified as major producers of the fecal pellets found in the trap throughout the study period. The acoustic time series from the moored AZFP showed that these taxa did not concentrate in the water layer above the trap, even after the inflow of AW and as irradiance increased and allowed pelagic primary production. The density of large copepods and euphausiids in the top 40 m of the water column represented $\sim$ 4% and 3% of their respective densities in the 40–82 m water layer right below the trap during the study period. Thus, only a small fraction of the population of large copepods and euphausiids were in the layer above the sediment trap throughout the entire study period (Fig. 4).

The presence of eggs and larvae indicates winter reproduction when food is a limiting factor for most plankton species. During the first half of the study period, the few eggs in the samples were most likely spawned by zooplankton detritivores, omnivores, and carnivores, such as *Microcalanus* spp. and *M. longa* who display active winter recruitment and do not rely entirely on primary production to fuel their reproduction (Hirche and Kosobokova 2011; Berge et al. 2015b). Dominance of the larval assemblage by the carnivore *C. limacina* in samples collected in January and February (Fig. 6) supports this assumption. The nature of the food source responsible for the increase in production of zooplankton fecal pellets and eggs in March-early April is difficult to trace based on the data at hand. The sensor installed at 37 m depth on the mooring line did not show any increase in fluorescence related to phytoplankton Chl *a* at that depth during the study period (Fig. 3). However, water sampling at 11 m depth by the Ferrybox system of the AWIPEV Underwater Long Term Fjord Observatory in Ny-Ålesund, revealed a steady but low increase in Chl *a* from late February to early April 2014, which was closely correlated with the daily PAR level (van de Poll et al. 2016). Furthermore, a recent study showed that phytoplankton sampled at the same AWIPEV coastal observatory, close to the mooring site in Kongsfjorden, was able to take advantage of the returning light to grow and accumulate biomass as early as February (Hoppe 2022). Thus, it is conceivable that pelagic primary production also began in February 2014, when PAR became sufficient in the surface layer, but at a low rate before environmental conditions, in particular stratification, were set for spring bloom development in May–June (Hegseth et al. 2019). Then, we can hypothesize that microzooplankton, mesozooplankton, and euphausiid grazers were feeding and controlled a developing but still moderate phytoplankton production near the surface, preventing it from

sinking to the depth of the moored fluorescence sensor. Furthermore, even species considered as primarily herbivorous, such as *Calanus* spp., and the krill *Thysanoessa inermis*, have flexible feeding strategies, switching to carnivory when microalgae become scarce (Kleppel 1993; Kunisch et al. 2023). Alternative food sources may include ciliates and heterotrophic protists (e.g., Nejstgaard et al. 1997; Levinsen et al. 2000; Campbell et al. 2009), as well as copepods eggs and nauplii (Basedow and Tande, 2006), which all can be abundant prior to the spring bloom in Svalbard fjords (Seuthe et al., 2011; Grenvald et al. 2016; Barth-Jensen et al. 2022).

Zooplankton-mediated particle export in winter–spring

In January–February, the $< 1.5 \, \mathrm{mg \, C \, m^{-2} \, d^{-1}}$ low FPC export fluxes at 40 m depth in central Kongsfjorden were within the range of fluxes measured during the same period at different depths within the top 110–0 m water layers of several Arctic regions, using various types of sediment traps (Table S2 in the Supporting Information). From March onward, the regular increase in FPC export reached a maximum of $20–31 \, \mathrm{mg \, C \, m^{-2} \, d^{-1}}$ in the last week of our study. These rates were > 20 times higher than FPC fluxes in the seasonally ice-covered Chukchi Sea at approximately the same season and depth, and comparable to fluxes on the Barents Sea shelf east of Svalbard during a late phytoplankton bloom phase in July 2003 (Wexels Riser et al. 2008; Table S2 in the Supporting Information).

In early April, carbon packaged as zooplankton fecal pellets appeared as the single component of the POC reaching the trap, indicating that zooplankton fecal pellet production can be a major source of organic carbon sinking out of the surface layer of high-Arctic fjord ecosystems during the late winter period. FPC : POC ratios > 100% (Table S2 in the Supporting Information) are most probably the result of FPC estimates based on mean volumetric carbon conversion factors established for different regions (southwestern Norwegian fjord, Beaufort Sea shelf and slope, eastern Svalbard shelf) and environmental conditions from winter to summer (Bodur et al. 2023). Nevertheless, our high FPC : POC ratios still support the key role of zooplankton processes in the export of POC in central Kongsfjorden after light becomes available again for photosynthesis, even before the main phytoplankton bloom (Fig. 3). Furthermore, the fact that this analysis did not consider fecal pellets < 60 μm in width makes the FPC estimates conservative to an unknown extent.

The pelagic food web was probably still in a detrital phase at the end of the polar night, as observed during the autumn and winter in the seasonally ice-covered slope of the Beaufort Sea and Franklin Bay in the western Canadian Arctic (Forest et al. 2007, 2008; Sampei et al. 2008). Small zooplankton detritivores and omnivores like *O. similis*, *Microcalanus* spp., oncaeid copepods, and microphagous appendicularians and *Limacina* spp. are more efficient feeders than the large *Calanus* grazers during the dark season of low and potentially poor-

quality food supply, when particles < 20 μm and detritus make the bulk of the organic matter available (Forest et al. 2007). However, the rather low C : N ratios (< 8) in late January indicated that the organic matter in the trap was relatively fresh prior to autochthonous primary production. The biomass of protists > 20 μm, dominated by ciliates, was low at the start of the study in January ($0.5–1.6 \, \mu\mathrm{g \, C \, L^{-1}}$, Grenvald et al. 2016), and possibly remained so until March (Seuthe et al. 2011). The sources of labile organic carbon that early in the year are not known. To better resolve the biological mechanisms that control the timing of the spring bloom in Kongsfjorden, and other coastal Arctic ecosystems influenced by AW, would require more high-resolution studies focusing on the prebloom period, such as ours.

The continuous decline in the C : N ratio throughout the study period (Fig. 8b) illustrated the gradual establishment of another food-web phase, defined by the accumulation of new POC, most likely through pelagic primary production (Hoppe 2022). A net positive primary production would have then started in the surface layer in late February-early March, at least 3 months before the peak of the phytoplankton bloom showed by the fluorescence measured at almost 40 m depth during the study period (Fig. 3) (van de Poll et al. 2016; Hegseth et al. 2019). From early March onward, improving food availability likely enhanced zooplankton fecal pellet production as indicated by the increase in FPC flux at 40 m depth, especially by the large *C. finmarchicus* and *C. glacialis* copepods, and *Thysanoessa* spp. which represented > 99% of the euphausiids in the fjord at that time (Grenvald et al. 2016). The rise in FPC export was mainly due to enhanced feeding activity rather than an increase in the abundance of large copepods and euphausiids in the surface layer in March–April (Fig. 4b,c).

In contrast to the significant role of euphausiids in the active transport of carbon to depth in Kongsfjorden (Darnis et al. 2017), their contribution to the gravitational export of POC was relatively low based on the two flux vectors investigated: FPC and exuviae. Euphausiid fecal pellets accounted for 14% of the zooplankton FPC export, compared with the 68% and 18% shares of the large and small–medium copepods, respectively, in March–April when FPC contributed predominantly to the POC export (Fig. 8d). Moreover, no euphausiid fecal pellets were observed in short-term traps deployed in January 2013, or in May, August, and October 2012 at different depths sampled at three sites in Kongsfjorden (Lalande et al. 2016). Furthermore, very few euphausiid fecal pellets were collected at 100 m depth during the January–April period in 2016 and 2017 in Kongsfjorden (Swoboda 2018). In previous studies conducted in the northeast Chukchi Sea, Beaufort Sea, and the northern Barents Sea, the euphausiid contribution to FPC export was not even considered (Forest et al. 2007, 2008; Wexels Riser et al. 2007; Sampei et al. 2008; Lalande et al. 2020). Carbon transported via sinking of euphausiid exuviae represented only 1% and 3.5% of the POC exported in March–April and over the entire study period, respectively. To

our knowledge, exuviae flux has so far not been measured in Arctic ecosystems. Manno et al. (2020) showed that the sinking of fecal pellets and exuviae produced by the euphausiid *Euphausia superba* can account for almost 90% of the annual POC export in the North Scotia Sea. But, there too, the euphausiid-mediated export remained low, especially under ice cover.

Methodological complementarity

A sediment trap is not a standard instrument to characterize zooplankton assemblages because the collection rate is sensitive to zooplankton behavior, in particular depth distribution, swimming activity, and vertical migration (Makabe et al. 2016). However, plankton net collections may also lead to under-sampling of the most active, smallest, or rarest species, or a potential bias related to sampling effort, mesh size, net clogging, and avoidance. For instance, the intact ellipsoidal fecal pellets in the trap samples in January revealed the presence of appendicularians in the surface layer, of which a few occasionally sank into the trap over the January-early March period (Fig. 5f). Conversely, the seven plankton net casts in January and May, did not catch any appendicularians near the mooring. Also notable was the large discrepancy in the ratio of small-medium to large copepods, 56 times higher in the plankton net samples than in the trap samples (Figs. 5a,c, 7a,b). The numerically dominant small species *O. similis*, *Pseudocalanus* spp. and *Microcalanus* spp. tend to perform limited, if any, vertical migrations compared with the larger *Calanus* species, known for their extensive diel and seasonal vertical migrations (Darnis and Fortier 2014). Thus, stationary traps should perform better at catching large mesozooplankton vertical migrators than small organisms that tend to keep to the surface layer even during winter (Søreide et al. 2022). Large zooplankton with stronger swimming capabilities might sense and avoid an upward moving net more efficiently than small organisms. However, we consider that the plankton nets used in this study provide reasonable estimates of relative abundances of large copepods, but surely not of macrozooplankton like euphausiids and amphipods. The zooplankton profiles illustrate well the discrepancy in the vertical distribution of the two size classes of copepods, as a major part of the large copepods remained below the trap depth in January and in May 2014, in contrast with the small-medium copepods concentrated in the top water layers (Fig. 7a,b,d,e). The high spatiotemporal resolution characterizing the acoustic sampling based on moored instruments can help a useful description of large zooplankton densities and vertical movements over time. However, in our case acoustic sampling was limited to a minor part of the water column (the top 80 m of a 203-m water column) in winter when large zooplankton are known to concentrate at depth. Furthermore, the AZFP acoustic data alone cannot help the taxonomic identification of the echoing particles. Our study demonstrates that combining data from nets, sequential sediment traps, and moored acoustic instruments can contribute to a better understanding of zooplankton dynamics over periods of weeks to months.

Conclusion

Darnis et al. (2017) showed that active transport via zooplankton DVM is a significant component of the biological carbon pump in winter in Kongsfjorden. The DVM-mediated carbon transport represented > 25% of the downward POC flux measured by our trap, and was largely due to euphausiid migration (Darnis et al. 2017). The present study further demonstrates the major influence of zooplankton activity on carbon pathways in the Kongsfjorden pelagic ecosystem by showing that sinking fecal pellets made the bulk of the POC export in late winter–spring. Large copepod grazers, such as *Calanus* spp., were mainly responsible for this passive flux of carbon. A thorough investigation of the role of zooplankton processes in the functioning of the biological carbon pump would need to also include the contribution of sinking carcasses from nonconsumptive mortality (Daase et al. 2014) and the active gut flux (release of fecal pellets after zooplankton DVM to the deep layer) during pre-bloom conditions in a carbon flux budget (Cavan et al. 2015; Dybwad et al. 2022). Dead zooplankton, mainly copepods, represented a non-negligible fraction (> 20%) of the zooplankton abundance in the plankton net samples collected in Svalbard fjords in January 2016 and 2017 (Daase and Søreide 2021). Thus, we could presume that a similar proportion of copepods caught in our trap were dead sinkers, not (live) swimmers, and their carbon content should have been tallied in the carbon export. However, distinguishing dead from live zooplankton in formalin-preserved samples remains a difficult task (Sampei et al. 2009). Sinking euphausiid carcasses were not an important means of carbon export out of the top 40 m of the water column during the present study period, based on the low number of individuals in the trap samples. Also, zooplankton processes that reduce the efficiency of the biological carbon pump should not be overlooked by future studies. These processes include the attenuation of the sinking export through the consumption (coprophagy) or mechanical degradation (coprorhexy) of sinking fecal pellets (Sampei et al. 2008), and algal grazing and carbon remineralization in the surface layer (Darnis and Fortier 2012). Despite the lack of information on primary production in the surface layer, our POC flux time series suggests a gradual development of the pelagic food web toward an autotrophic phase from winter to spring, most probably stimulated by increasing light availability. Because prebloom biological activity in western Svalbard fjords is higher than previously thought, future research should address more thoroughly the winter processes that link AW inflow events, phytoplankton activity, and trophic interactions within the pelagic food web, not to mention the benthic/pelagic coupling, if we are to properly anticipate the responses of these

high-Arctic marine ecosystems to the double impact of climate warming and intensified Atlantification.

Data availability statement

The data supporting this study are available in the Supporting Information Material of this article.

References

Ardyna, M., and others. 2020. Under-ice phytoplankton blooms: Shedding light on the "invisible" part of arctic primary production. Front. Mar. Sci. **7**: 1–25. doi:10.3389/fmars.2020.608032

ASL. 2014. AZFP (acoustic zooplankton fish profiler) operators manual. ASL, p. 77.

Barth-Jensen, C., M. Daase, M. Ormańczyk, Ø. Varpe, S. Kwasniewski, and C. Svensen. 2022. High abundances of small copepods early developmental stages and nauplii strengthen the perception of a non-dormant arctic winter. Polar Biol. **45**: 675–690. doi:10.1007/s00300-022-03025-4

Basedow, S. L., K. Eiane, V. Tverberg, and M. Spindler. 2004. Advection of zooplankton in an Arctic fjord (Kongsfjorden, Svalbard). Estuar. Coast. Shelf Sci. **60**: 113–124. doi:10.1016/j.ecss.2003.12.004

Basedow, S. L., A. Sundfjord, W.-J. von Appen, E. Halvorsen, S. Kwasniewski, and M. Reigstad. 2018. Seasonal variation in transport of zooplankton into the Arctic Basin through the Atlantic gateway. Fram Strait. Front. Mar. Sci. **5**: 1–22. doi:10.3389/fmars.2018.00194

Basedow, S., and K. Tande. 2006. Cannibalism by female Calanus finmarchicus on naupliar stages. Marine Ecology Progress Series **327**: 247–255. doi:10.3354/meps327247

Berge, J., and others. 2015*a*. Unexpected levels of biological activity during the polar night offer new perspectives on a warming Arctic. Curr. Biol. **25**: 2555–2561. doi:10.1016/j.cub.2015.08.024

Berge, J., and others. 2015*b*. In the dark: A review of ecosystem processes during the Arctic polar night. Prog. Oceanogr. **139**: 258–271. doi:10.1016/j.pocean.2015.08.005

Berge, J., G. Johnsen, and J. Cohen. 2020. Polar night marine ecology. Life and light in the dead of night. Springer Cham, p. 375. doi:10.1007/978-3-030-33208-2

Bodur, Y. V., and others. 2023. Seasonal patterns of vertical flux in the northwestern Barents Sea under Atlantic water influence and sea-ice decline. Prog. Oceanogr. **219** (103132): 1–14. doi:10.1016/j.pocean.2023.103132

Campbell, R. G., E. B. Sherr, C. J. Ashjian, S. Plourde, B. F. Sherr, V. Hill, and D. A. Stockwell. 2009. Mesozooplankton prey preference and grazing impact in the western Arctic Ocean. Deep Sea Res. Part II Top. Stud. Oceanogr. **56**: 1274–1289. doi:10.1016/j.dsr2.2008.10.027

Cavan, E. L., F. A. C. Le Moigne, A. J. Poulton, G. A. Tarling, P. Ward, C. J. Daniels, G. M. Fragoso, and R. J. Sanders. 2015.

Attenuation of particulate organic carbon flux in the Scotia Sea, Southern Ocean, is controlled by zooplankton fecal pellets. Geophys. Res. Lett. **42**: 821–830. doi:10.1002/2014GL062744

Cohen, J. H., and others. 2015. Is ambient light during the high Arctic polar night sufficient to act as a visual cue for zooplankton? PLoS One **10**: e0126247. doi:10.1371/journal.pone.0126247

Daase, M., Ø. Varpe, and S. Falk-Petersen. 2014. Non-consumptive mortality in copepods: Occurrence of Calanus spp. carcasses in the Arctic Ocean during winter. J. Plankton Res. **36**: 129–144. doi:10.1093/plankt/fbt079

Daase, M., and J. E. Søreide. 2021. Seasonal variability in non-consumptive mortality of Arctic zooplankton. J. Plankton Res. **43**: 565–585. doi:10.1093/plankt/fbab042

Darnis, G., and L. Fortier. 2012. Zooplankton respiration and the export of carbon at depth in the Amundsen gulf (Arctic Ocean). J. Geophys. Res. Oceans **117**: C04013. doi:10.1029/2011JC007374

Darnis, G., and L. Fortier. 2014. Temperature, food and the seasonal vertical migration of key arctic copepods in the thermally stratified Amundsen gulf (Beaufort Sea, Arctic Ocean). J. Plankton Res. **36**: 1092–1108. doi:10.1093/plankt/fbu035

Darnis, G., and others. 2017. From polar night to midnight sun: Diel vertical migration, metabolism and biogeochemical role of zooplankton in a high arctic fjord (Kongsfjorden, Svalbard). Limnol. Oceanogr. **62**: 1586–1605. doi:10.1002/lno.10519

Dybwad, C., and others. 2022. The influence of sea ice cover and Atlantic water advection on annual particle export north of Svalbard. J. Geophys. Res. Oceans. **127**: e2022JC018897. doi:10.1029/2022JC018897

Forest, A., M. Sampei, H. Hattori, R. Makabe, H. Sasaki, M. Fukuchi, P. Wassmann, and L. Fortier. 2007. Particulate organic carbon fluxes on the slope of the Mackenzie shelf (Beaufort Sea): Physical and biological forcing of shelf-basin exchanges. J. Mar. Syst. **68**: 39–54. doi:10.1016/j.jmarsys.2006.10.008

Forest, A., M. Sampei, R. Makabe, H. Sasaki, D. G. Barber, Y. Gratton, P. Wassmann, and L. Fortier. 2008. The annual cycle of particulate organic carbon export in Franklin Bay (Canadian Arctic): Environmental control and food web implications. J. Geophys. Res. Oceans. **113**. 1–14. doi:10.1029/2007JC004262

Fortier, L., J. Le Fèvre, and L. Legendre. 1994. Export of biogenic carbon to fish and to the deep ocean: The role of large planktonic microphages. J. Plankton Res. **16**: 809–839. doi:10.1093/plankt/16.7.809

González, H. E., S. R. González, and G.-J. Brummer. 1994. Short-term sedimentation pattern of zooplankton, faeces and microplankton at a permanent station in the Bjornafjorden (Norway) during April-may 1992. Mar. Ecol. Prog. Ser. **105**: 31–45.

González, H. E., and V. Smetacek. 1994. The possible role of the cyclopoid copepod *Oithona* in retarding vertical flux of zooplankton faecal material. Mar. Ecol. Prog. Ser. **113**: 233–246.

Grenvald, J. C., and others. 2016. Plankton community composition and vertical migration during polar night in Kongsfjorden. Polar Biol. **39**: 1879–1895. doi:10.1007/s00300-016-2015-x

Halfter, S., E. L. Cavan, K. M. Swadling, R. S. Eriksen, and P. W. Boyd. 2020. The role of zooplankton in establishing carbon export regimes in the Southern Ocean–A comparison of two representative case studies in the subantarctic region. Front. Mar. Sci. **7**: 1–8. doi:10.3389/fmars.2020.567917

Hegseth, E. N., and other. 2019. Phytoplankton seasonal dynamics in Kongsfjorden, Svalbard and the adjacent shelf, p. 173–227. *In* H. Hop and C. Wiencke [eds.], The ecosystem of Kongsfjorden, Svalbard. Springer International Publishing. doi:10.1007/978-3-319-46425-1_6

Hirche, H. J., and K. N. Kosobokova. 2011. Winter studies on zooplankton in Arctic seas: The Storfjord (Svalbard) and adjacent ice-covered Barents Sea. Mar. Biol. **158**: 2359–2376. doi:10.1007/s00227-011-1740-5

Hop, H., and others. 2002. The marine ecosystem of Kongsfjorden, Svalbard. Polar Res. **21**: 167–208. doi:10.3402/polar.v21i1.6480

Hop, H., and C. Wiencke. 2019. The ecosystem of Kongsfjorden, Svalbard. Springer International Publishing, p. 1–20. doi:10.1007/978-3-319-46425-1_1

Hop, H., and others. 2019. Zooplankton in Kongsfjorden (1996–2016) in relation to climate change, p. 229–300. *In* H. Hop and C. Wiencke [eds.], The ecosystem of Kongsfjorden, Svalbard. Springer International Publishing. doi:10.1007/978-3-319-46425-1_7

Hoppe, C. J. M. 2022. Always ready? Primary production of arctic phytoplankton at the end of the polar night. Limnol. Oceanogr. Lett. **7**: 167–174. doi:10.1002/lol2.10222

Jónasdóttir, S. H., A. W. Visser, K. Richardson, and M. R. Heath. 2015. Seasonal copepod lipid pump promotes carbon sequestration in the deep north Atlantic. Proc. Natl. Acad. Sci. **112**: 12122–12126. doi:10.1073/pnas.151211011

Kiko, R., D. Bianchi, C. Grenz, H. Hauss, M. Iversen, S. Kumar, A. Maas, and C. Robinson. 2020. Editorial: Zooplankton and nekton: Gatekeepers of the biological pump. Front. Mar. Sci. **7**: 1–2. doi:10.3389/fmars.2020.00545

Kleppel, G. S. 1993. On the diets of calanoid copepods. Marine Ecology Progress Series. **99**: 183–195.

Kunisch, E. H., M. Graeve, R. Gradinger, H. Flores, Ø. Varpe, and B. A. Bluhm. 2023. What we do in the dark: Prevalence of omnivorous feeding activity in Arctic zooplankton during polar night. Limnology and Oceanography **68**: 1835–1851. Portico. doi:10.1002/lno.12389

Lalande, C., B. Moriceau, A. Leynaert, and N. Morata. 2016. Spatial and temporal variability in export fluxes of biogenic matter in Kongsfjorden. Polar Biol. **39**: 1725–1738. doi:10.1007/s00300-016-1903-4

Lalande, C., J. M. Grebmeier, R. R. Hopcroft, and S. L. Danielson. 2020. Annual cycle of export fluxes of biogenic matter near Hanna shoal in the northeast Chukchi Sea. Deep Sea Res. Part II Top. Stud. Oceanogr. **177**: 104730. doi:10.1016/j.dsr2.2020.104730

Levinsen, H., J. Turner, T. Nielsen, and B. Hansen. 2000. On the trophic coupling between protists and copepods in arctic marine ecosystems. Marine Ecology Progress Series **204**: 65–77. doi:10.3354/meps204065

Makabe, R., H. Hattori, M. Sampei, G. Darnis, L. Fortier, and H. Sasaki. 2016. Can sediment trap-collected zooplankton be used for ecological studies? Polar Biol. **39**: 2335–2346. doi:10.1007/s00300-016-1900-7

Manno, C., S. Fielding, G. Stowasser, E. J. Murphy, S. E. Thorpe, and G. A. Tarling. 2020. Continuous moulting by Antarctic krill drives major pulses of carbon export in the north Scotia Sea, Southern Ocean. Nat. Commun. **11**: 6051. doi:10.1038/s41467-020-19956-7

Nejstgaard, J., I. Gismervik, and P. Solberg. 1997. Feeding and reproduction by Calanus finmarchicus, and microzooplankton grazing during mesocosm blooms of diatoms and the coccolithophore Emiliania huxleyi. Marine Ecology Progress Series **147**: 197–217. doi:10.3354/meps147197

Oziel, L., A. Baudena, M. Ardyna, P. Massicotte, A. Randelhoff, J. B. Sallée, R. B. Ingvaldsen, E. Devred, and M. Babin. 2020. Faster Atlantic currents drive poleward expansion of temperate phytoplankton in the Arctic Ocean. Nat. Commun. **11**: 1705. doi:10.1038/s41467-020-15485-5

van de Poll, W., D. Maat, P. Fischer, P. Rozema, O. Daly, S. Koppelle, R. Visser, and A. Buma. 2016. Atlantic advection driven changes in glacial meltwater: Effects on phytoplankton chlorophyll-a and taxonomic composition in Kongsfjorden, Spitsbergen. Front. Mar. Sci. **3**: 1–11. doi:10.3389/fmars.2016.00200

Polyakov, I. V., and others. 2020. Borealization of the Arctic Ocean in response to anomalous advection from sub-arctic seas. Front. Mar. Sci. **7**: 1–32. doi:10.3389/fmars.2020.0049

Randelhoff, A., and others. 2020. Arctic mid-winter phytoplankton growth revealed by autonomous profilers. Sci. Adv. **6**: eabc2678. doi:10.1126/sciadv.abc2678

Rantanen, M., A. Y. Karpechko, A. Lipponen, K. Nordling, O. Hyvärinen, K. Ruosteenoja, T. Vihma, and A. Laaksonen. 2022. The arctic has warmed nearly four times faster than the globe since 1979. Commun. Earth Environ. **3**: 168. doi:10.1038/s43247-022-00498-3

Sampei, M., A. Forest, H. Sasaki, H. Hattori, R. Makabe, M. Fukuchi, and L. Fortier. 2008. Attenuation of the vertical flux of copepod fecal pellets under arctic sea ice: Evidence for an active detrital food web in winter. Polar Biol. **32**: 225–232. doi:10.1007/s00300-008-0523-z

Sampei, M., H. Sasaki, H. Hattori, A. Forest, and L. Fortier. 2009. Significant contribution of passively sinking copepods to downward export flux in Arctic waters. Limnol. Oceanogr. **54**: 1894–1900. doi:10.4319/lo.2009.54.6.1894

Seuthe, L., G. Darnis, C. Wexels Riser, P. Wassmann, and L. Fortier. 2007. Winter–spring feeding and metabolism of arctic copepods: Insights from faecal pellet production and respiration measurements in the southeastern Beaufort Sea. Polar Biol. **30**: 427–436. doi:10.1007/s00300-006-0199-1

Seuthe, L., K. Rokkan Iversen, and F. Narcy. 2011. Microbial processes in a high-latitude fjord (Kongsfjorden, Svalbard): II. Ciliates and dinoflagellates. Polar Biol. **34**: 751–766. doi:10.1007/s00300-010-0930-9

Shu, Q., Q. Wang, M. Årthun, S. Wang, Z. Song, M. Zhang, and F. Qiao. 2022. Arctic Ocean amplification in a warming climate in cmip6 models. Sci. Adv. **8**: eabn9755. doi:10.1126/sciadv.abn9755

Søreide, J. E., K. Dmoch, K. Blachowiak-Samolyk, E. Trudnowska, and M. Daase. 2022. Seasonal mesozooplankton patterns and timing of life history events in high-arctic fjord environments. Frontiers in Marine Science **9**. doi:10.3389/fmars.2022.933461

Stanton, T. K., P. H. Wiebe, D. Chu, M. C. Benfield, L. Scanlon, L. Martin, and R. L. Eastwood. 1994. On acoustic estimates of zooplankton biomass. ICES J. Mar. Sci. **51**: 505–512. doi:10.1006/jmsc.1994.1051

Svendsen, H., and others. 2002. The physical environment of Kongsfjorden–Krossfjorden, an Arctic fjord system in Svalbard. Polar Res. **21**: 133–166. doi:10.1111/j.1751-8369.2002.tb00072.x

Swoboda, S. 2018. The annual cycle of particle flux in sea ice influenced and ice-free Arctic fjords. UNIS The Univ. Centre Svalbard.

Tremblay, J.-É., and others. 2006. Trophic structure and pathways of biogenic carbon flow in the eastern north water polynya. Prog. Oceanogr. **71**: 402–425. doi:10.1016/j.pocean.2006.10.006

Tverberg, V., and others. 2019. The Kongsfjorden transect: Seasonal and inter-annual variability in hydrography, p. 49–104. *In* H. Hop and C. Wiencke [eds.], The ecosystem of Kongsfjorden, Svalbard. Springer International Publishing. doi:10.1007/978-3-319-46425-1_3

Wexels Riser, C., M. Reigstad, P. Wassmann, E. Arashkevich, and S. Falk-Petersen. 2007. Export or retention? Copepod

abundance, faecal pellet production and vertical flux in the marginal ice zone through snap shots from the northern Barents Sea. Polar Biol. **30**: 719–730. doi:10.1007/s00300-006-0229-z

Wexels Riser, C., P. Wassmann, M. Reigstad, and L. Seuthe. 2008. Vertical flux regulation by zooplankton in the northern Barents Sea during arctic spring. Deep Sea Res Part II Top. Stud. Oceanogr. **55**: 2320–2329. doi:10.1016/j.dsr2.2008.05.006

Weydmann, A., P. Prątnicka, M. Łącka, S. Majaneva, F. Cottier, and J. Berge. 2021. Zooplankton and sediment fluxes in two contrasting fjords reveal Atlantification of the Arctic. Sci. Tot. Environ. **773**: 145599. doi:10.1016/j.scitotenv.2021.145599

Willis, K., F. Cottier, and S. Kwasniewski. 2008. Impact of warm water advection on the winter zooplankton community in an Arctic fjord. Polar Biol. **31**: 475–481. doi:10.1007/s00300-007-0373-0

Conflict of Interest

None declared.